THE JOURNAL OF PHYSICAL CHEMISTRY A

ARTICLE

pubs.acs.org/JPCA

Detailed Mechanism for Photoinduced Cytosine Dimerization: A Semiclassical Dynamics Simulation

Shuai Yuan,[†,‡] Wenying Zhang,[‡] Lihong Liu,[†] Yusheng Dou,[‡,§,*] Weihai Fang,[†,*] and Glenn V. Lo[§]

[†]Department of Chemistry, Beijing Normal University, Beijing 100875, China

[‡]College of Bio-information, Chongqing University of Posts and Telecommunications, Chongqing 400065, China

[§]Department of Physical Sciences, Nicholls State University, P.O. Box 2022, Thibodaux, Louisiana 70310, United States

ABSTRACT: Semiclassical dynamics simulation is used to study dimerization of two stacked cytosine molecules following excitation by ultrashort laser pulses (25 fs fwhm, Gaussian, 4.1 eV photon energy). The initial excited state was found to form an ultrashort exciton state, which eventually leads to the formation of an excimer state by charge transfer. When the interbase distance, defined as an average value of C_5-C_5' and C_6-C_6', becomes less than 3 Å, charge recombination occurs due to strong intermolecular interaction, eventually leading to an avoided crossing within 20−30 fs. Geometries at the avoided crossing, with average intermolecular distance of about 2.1 Å, are in accord with CASSCF/CASPT2 calculations. Results indicate that the $C_2-N_1-C_6-C_5$ and $C_2'-N_1'-C_6'-C_5'$ dihedral angles' bending vibrations play a significant role in the vibronic coupling between the HOMO and LUMO, which leads to a nonadiabatic transition to the electronic ground state.

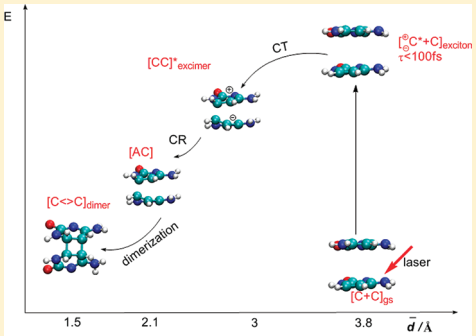

Mechanism of photodimerization reaction of π stacked cytosines system.

I. INTRODUCTION

UV radiation is widely regarded as a major environmental mutagenic agent. Exposure of DNA to UV radiation causes DNA damage.[1] Most photoinduced lesions involve the formation of cyclobutane pyrimidine dimers (CPDs) between adjacent pyrimidine bases within the same DNA strand.[2,3] The formation of CPDs is considered as the main cause of cell death, mutagenesis, and development of skin cancers.[4] Intensive experimental[5−8] and theoretical[9−12] investigations have focused on CPDs since their discovery about fifty years ago.[2]

The thymine dimer (T<>T) is the major CPD induced in DNA by UV radiation, but the cytosine dimer (C<>C) is more likely to cause mutation.[13,14] In fact, the initially formed CPDs are not significantly mutagenic because living organisms can effectively repair the photodamage by catalytic action of DNA photolyase enzyme, resulting in the cleavage of the C_5-C_5' and C_6-C_6' bonds of the pyrimidine dimers. However, deamination derivatives of cytosine are highly mutagenic to genes.[15] The C<>C and 5-methylcytosine (5mC<>5mC) dimers deaminate to uracil and thymine in a matter of hours or days,[16] unlike their canonical forms, which deaminate with a half-life of about 50 000 years.[17]

Experimental fluorescence spectra suggest that the excited-state dynamics of base multimers are radically different from those of the constituent nucleotides. In polynucleotides, a long-lived, red-shifted emissive excited state[18] with charge transfer (CT)[19] characteristic was observed more than forty years ago. The red-shifted emission was first assigned to an excimer by Eisinger.[18] The excited state of stacked base multimer shows multiexponential decays with very different time constants.[20−28] For instance, time-resolved studies[26] on $(dA)_{20}$ provide three different signals with time scales of 0.39, 4.3, and 182 ps. Crespo-Hernández and Kohler et al.[27,28] attributed the long-lived states observed in single-stranded oligonucleotides to an intrastrand excimer/exciplex resulting from π-stacking of an excited base with an adjacent unexcited base. They also claimed that the fast and slow signal components correspond to excitations in unstacked and stacked base regions, respectively.[27] It can be deduced that the stacking-dependent excited state lifetime of the purine dimer is longer than that of the prymidine dimer. Results of femtosecond time-resolved fluorescence spectroscopy have shown that lifetimes of the electronic excited state in the pyrimidine single-stranded molecules $d(T)_{20}$, $d(TTCTT)_4$, $dT(TCT)_6T$, $d(TC)_{10}$, $d(TC)_9T$, $d(C)_{20}$, and $d(C)_{10}$ are slightly longer but still similar to those of the monomeric nucleotides, which are less than 1 ps.[29] This finding leads to the conclusion that pyrimidine-base single strands do not generally form super long-lived excimer/exciplex states.

The Frenkel exciton model was used in much theoretical work on DNA to explain the long-lived excited states.[30−33] A recent review[28] states that an exciton state decays to an exciplex state in less than 1 ps and the exciplex state returns to the ground state on a time scale of 10−100 ps via charge recombination. These results established the importance of charge-transfer quenching pathways as a decay channel for UV-irradiated DNA. The longer lifetimes are attributed to interbase charge transfer (CT)

Received: August 6, 2011
Revised: October 11, 2011
Published: October 11, 2011

states,[27,34−38] due to a transfer of energy from one base to its π-stacked neighbor.

Different mechanisms have been proposed for pyrimidine dimer production via singlet and triplet states, respectively. High-level ab initio studies[9,12] have indicated that the thymine dimerization occurs along a singlet potential surface and reaches a conical intersection $(S_1/S_0)_{CI}$ through a barrierless concerted nonadiabatic pathway. The $(S_1/S_0)_{CI}$ is a funnel of ultrafast nonradiative deactivation leading to the formation of T<>T. Our recent dynamics simulation,[39] however, indicated that the T<>T are formed asynchronously due to the C_5-C_5' distance being longer than C_6-C_6' at the avoided crossing. Roca-Sanjuán et al. proposed[40,41] that C<>C photodimer formation is mediated along the triplet and singlet manifold by a singlet−triplet crossing, $(T_1/S_0)_X$, and by a conical intersection, $(S_1/S_0)_{CI}$, respectively, on the basis of CASPT2 calculation. They also found that the quantum yield of C<>C dimerization is low compared to T<>T because the former has to surmount a barrier of 0.2 eV from excimer state to $(S_1/S_0)_{CI}$ whereas the latter has a barrierless channel.

A singlet excimer has been suggested to be a precursor to C<>C photodimerization, but the origin and mechanisms of both excimer and photodimer formations at the molecular level are controversial and poorly understood. How the initial excited state converts to excimer and the detailed CT process are still unresolved. The deactivation mechanisms of the relatively shorter prymidine excimer and base monomer can hardly be distinguished experimentally.

Despite the importance of DNA photostability and photodamage and the intense work in the field, the molecular dynamics study is still poorly understood. Understanding a chemical reaction ultimately requires the knowledge of how each atom in the reactant molecules moves during product formation. Such knowledge is seldom complete and is often limited to an oversimplified reaction coordinate that neglects global motion across the molecular framework. To overcome this limit, we used the semiclassical electron-radiation-ion dynamics (SERID) method to describe variations of every reaction coordinate and energy versus time in this paper. The simulation results provide detailed dynamics features for this process from photon excitation to the formation of product.

II. METHODOLOGY

The SERID method is used to carry out dynamics simulations. This technique is described in detail elsewhere.[42,43] In this methodology, the valence electrons are calculated by the time-dependent Schrödinger equation whereas both the radiation field and the motion of the nuclei are treated classically. The one-electron states are obtained for each time step by solving the time-dependent Schrödinger equation in a nonorthogonal basis,

$$i\hbar\frac{\partial\Psi_j}{\partial t} = \mathbf{S}^{-1}\cdot H\cdot\Psi_j \tag{1}$$

where $\mathbf{S}$ is the overlap matrix of the atomic orbitals. The laser pulse is characterized by the vector potential $\mathbf{A}$, which is coupled to the Hamiltonian via the time-dependent Peierls substitution[44]

$$H_{ab}(\mathbf{X}-\mathbf{X}') = H^0_{ab}(\mathbf{X}-\mathbf{X}')\exp\left\{\frac{iq}{\hbar c}A\cdot(\mathbf{X}-\mathbf{X}')\right\} \tag{2}$$

where $H_{ab}(\mathbf{X}-\mathbf{X}')$ is the Hamiltonian matrix element for basis functions a and b on atoms at $\mathbf{X}$ and $\mathbf{X}'$, respectively, and $q = -e$ is the charge of the electron.

In SERID, forces acting on nuclei or ions are computed by the Ehrenfest equation:

$$M_l\frac{d^2X_{la}}{dt^2} = -\frac{1}{2}\sum_j \Psi_j^+\cdot\left(\frac{\partial H}{\partial X_{la}} - i\hbar\frac{1}{2}\frac{\partial S}{\partial X_{la}}\cdot\frac{\partial}{\partial t}\right)\cdot\Psi_j - \frac{\partial U_{rep}}{\partial X_{la}} \tag{3}$$

where U_{rep} is effective nuclear−nuclear repulsive potential and $X_{la} = \langle\hat{X}_{la}\rangle$ is the expectation value of the time-dependent Heisenberg operator for the α coordinate of the nucleus labeled by l (with $\alpha = x, y, z$). Equation 3 is obtained by neglecting the second and higher order terms of the quantum fluctuations $\hat{X} - \langle\hat{X}_{la}\rangle$ in the exact Ehrenfest theorem.

The time-dependent Schrödinger equation (1) is solved by using a unitary algorithm obtained from the equation for the time evolution operator.[45] Equation 3 is numerically integrated with the velocity Verlet algorithm. A time step of 0.05 fs is used for this study and energy conservation was then found to hold better than 1 part in 10^6 in a 1 ps simulation at 298 K.

The present "Ehrenfest" principle is complementary to other methods based on different approximations, such as the full multiple spawning model developed by the Martinez group.[46] The limitation of this method is that the simulation trajectory moves along a path dominated by averaging over all the terms in the Born−Oppenheimer expansion,

$$\Psi^{total}(X_n, x_e, t) = \sum_j \Psi_i^n(X_n, t)\,\Psi_i^e(x_e, X_n) \tag{4}$$

rather than following the time evolution of a single potential energy surface, which is approximately decoupled from all the others. (Here X_n and x_e represent the sets of nuclear and electronic coordinates respectively, and the Ψ_i^e are eigenstates of the electronic Hamiltonian at fixed X_n.) The strengths of the present approach include the retention of all of the $3N$ nuclear degrees of freedom and incorporation of both the excitation due to a laser pulse and the subsequent de-excitation at an avoided crossing near a conical intersection.

SERID has been used to study several photochemical reactions and was found to yield good descriptions of molecular response to ultrashort laser pulses. The examples include that the calculation of the photoisomerization mechanism of azobenzene[47−51] for nπ^* and $\pi\pi^*$ excitations. The method has also been used in biologically relevant studies such as nonadiabatic decay for adenine,[52] photodissociation of cyclobutane thymine dimer[53] and photoinduced dimerization of thymine,[39] and deactivation via long-lived excimers of stacked adenines.[54,55] All the results were found to be consistent with experimental observations.

III. RESULTS AND DISCUSSION

A dynamics simulation was run for a ground-state cytosine at room temperature (298 K) for 2000 fs. A second cytosine molecule of the same geometry is oriented such that C_5-C_5' = 3.45 Å, C_6-C_6' = 3.43 Å, and $C_5-C_6-C_6'-C_5'$ = 26.4°; primed labels refer to atoms of the second ground-state cytosine molecule. This is essentially the same configuration for the cyclobutane thymine dimer in an earlier study.[9,12] The simulation was continued for another 2000 fs. Twenty structures at 200 fs intervals were recorded. The structure at 1000 fs is shown in

Figure 1, where the two molecules are stacked such that the interatomic distances (C_5-C_5') and (C_6-C_6') are 3.85 and 3.90 Å, respectively, and the dihedral angle ($C_4-C_5-C_5'-C_4'$) is 36.1°. Each of the twenty structures is used as the starting geometry for a simulated trajectory initiated by laser excitation. In the following discussion, the excited cytosine molecule will be referred to as molecule C and the other unexcited molecule will be referred to as C′.

A 25 fs fwhm laser pulse with a Gaussian profile and photon energy of 4.1 eV was used in the simulations. The selected photon energy corresponds to the energy gap between the LUMO and HOMO, as calculated by the present approximation and is about halfway between the experimental photon energies (290−320 nm) used in experimental studies.[1,15] A fluence of 100−300 J/m^2 was chosen for this study. This fluence results in an effective electronic excitation, but the forces produced do not break any bonds. The simulation was run at the selected laser pulse for 500 trajectories and only a typical trajectory is reported in this paper because other trajectories have shown similar properties.

Six snapshots taken from the representative trajectory at different times are shown in Figure 2. The geometry at the point of laser excitation is shown in Figure 2a; only the top cytosine molecule (C) is excited. The excited molecule distorts and moves toward its unexcited neighbor, C′ (Figure 2b). Intermolecular forces lead to deformation of C′ (Figure 2c). By 848 fs, the C_6 and C_6' atoms are covalently bonded (Figure 2d); 10 fs later, the C_5-C_5' bond is formed (Figure 2e). In other words, the formation of cyclobutane pyrimidine dimer is essentially concerted. The structure of cyclobutane pyrimidine dimer remains stable through the end of the simulation (Figure 2f).

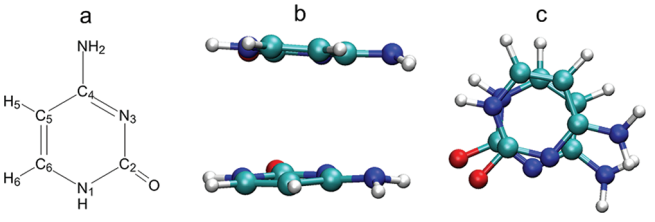

Figure 1. Structure and atomic labeling for the stacked cytosine molecules.

The variations with time of the HOMO−1, HOMO, LUMO, and LUMO+1 energies and the time-dependent population of those four orbitals are shown in Figure 3a,b, respectively. Figure 3a shows that there is an abrupt fall in the LUMO energy soon after the application of the laser pulse. An intersection between the HOMO and LUMO levels, an avoided crossing induced by coupling of orbitals, with the energy gaps of 0.04 eV is found at 830 fs. Figure 3b shows that by the end of the laser pulse

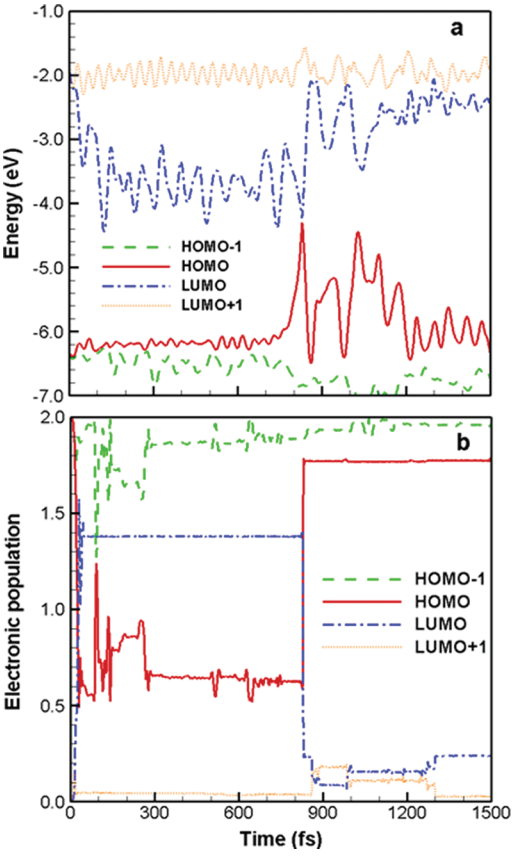

Figure 3. (a) Variations with time and (b) the time-dependent populations of the HOMO−1, HOMO LUMO, and LUMO+1 energies of two stacked cytosine molecules.

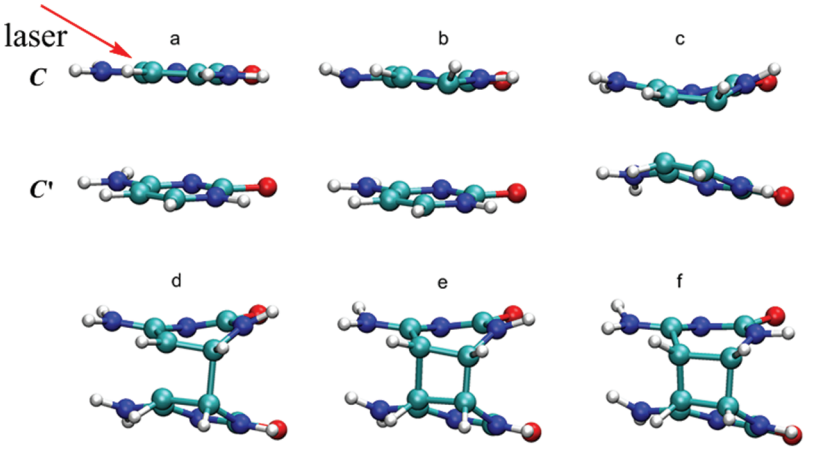

Figure 2. Snapshots taken from the simulation of two stacked cytosine molecules at (a) 0, (b) 400, (c) 827, (d) 847, (e) 858, and (f) 1000 fs. The molecule at the top is subjected to irradiation by a 25 fs (fwhm) laser pulse with a fluence of 83.62 J/m^2 and photon energy of 4.1 eV.

dx.doi.org/10.1021/jp207550a |J. Phys. Chem. A 2011, 115, 13291–13297

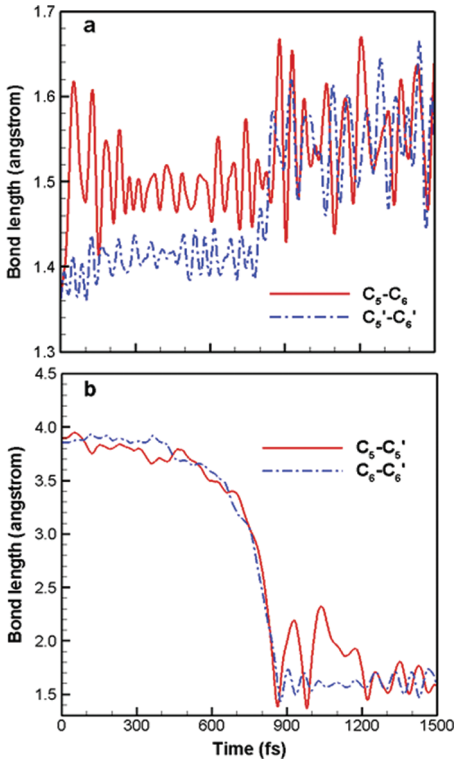

Figure 4. (a) Variations with time of the lengths between the C_5 and C_6 atoms and the C_5' and C_6' atoms. (b) Variations with time of the lengths between the C_5 and C_5' atoms and the C_6 and C_6' atoms in two stacked cytosines molecules.

radiation (which is 50 fs) about 1.4 electrons are excited from the HOMO to the LUMO, which promotes one cytosine molecule to an electronically excited state. The coupling between the HOMO and LUMO, as observed in Figure 3a, suggests electronic transition from the LUMO to the HOMO. This de-excitation ultimately brings the molecules to the electronic ground state. It can be seen from Figure 3a that shortly after the coupling both the LUMO and HOMO levels move toward their initial values. After 900 fs, when the formation of the cyclobutane pyrimidine dimer is completed, these two energy levels slightly fluctuate about constant values that are essentially the same as their initial values. The excited state lifetime of 780 fs is about 2−3 times that for nonadiabatic deactivation of cytosine monomer.[56]

The variations with time of the lengths of the C_5-C_6, $C_5'-C_6'$, C_5-C_5', and C_6-C_6' bonds are presented in Figure 4. Both C_5-C_6 and $C_5'-C_6'$ are double bonds at the beginning of simulation but convert to single σ bonds in the cyclobutane pyrimidine dimer (Figure 4a). Starting at about 1.38 Å, which is the length of a typical C−C double bond in conjugated aromatic system, the C_5-C_6 bond length elongates to about 1.5 Å after the laser pulse applied whereas the $C_5'-C_6'$ bond length remains essentially constant. The excited cytosine molecule approaches its unexcited neighbor and the geometry of the latter changes obviously, as shown by the increase in the $C_5'-C_6'$ bond length after 800 fs. The $C_5'-C_6'$ bond length increases to about 1.5 Å after 850 fs because of the formation of the cyclobutane pyrimidine dimer and remains at this length until the end of the simulation. In Figure 4b, both C_5-C_5' and C_6-C_6' distances are more or less constant up to 100 fs. The C_5-C_5' and C_6-C_6' distances decrease to below 1.5 Å at about 850 and 860 fs,

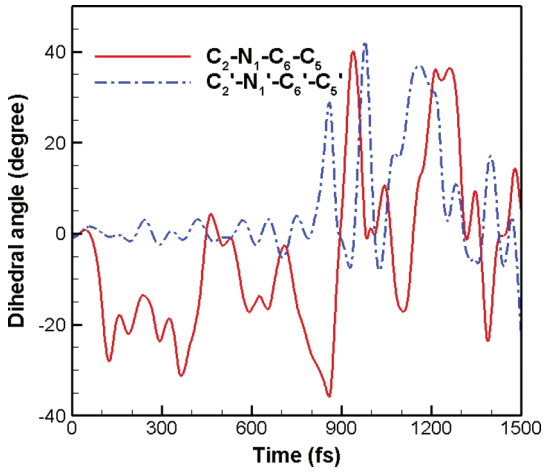

Figure 5. Variations with time of the dihedral angles $C_2-N_1-C_6-C_5$ and $C_2'-N_1'-C_6'-C_5'$ of two stacked cytosines.

respectively. The experimental value for the formation time of the cyclobutane cytosine dimer is not available. However, the value obtained by the simulation is very similar to the experimental observations for the T<>T dimer[29] and also agrees well with one from other theoretical calculations.[9,11,40,41,57]

Photoinduced [2+2] cycloaddition reactions proceed via a cyclic transition state and are concerted reactions in which bond breaking and bond formation take place simultaneously and no intermediate state is involved. For the photoinduced dimerization of cytosines, cycloaddition results in the conversion of C_5-C_6 and $C_5'-C_6'$ π-bonds, one on each pyrimidine ring, into two σ-bonds of the cyclobutane ring (C_5-C_5' and C_6-C_6' bonds). CASSCF calculation[40] suggests that in the photochemical [2+2] cycloaddition, two stacked cytosines decay to the electronic ground state via the conical intersection before the formation of the C_5-C_5' and C_6-C_6' bonds and that at the conical intersection, the C_5-C_5' distance is just slightly longer than the C_6-C_6' distance. It is therefore inferred that the C_5-C_5' and C_6-C_6' bond formations are asynchronous. This inference is consistent with our simulation results.

The variations of dihedral angles, $C_2-N_1-C_6-C_5$ and $C_2'-N_1'-C_6'-C_5'$, which describe the twisting of the C_5-C_6 and $C_5'-C_6'$ bonds, respectively, are shown in Figure 5. The dihedral $C_2-N_1-C_6-C_5$ decreases from 0° to −28° within 120 fs and then fluctuates around an average value of −20°. It indicates that the C molecule has been deformed due to excitation. This angle reaches a maximum of −35° at 860 fs and returns to its initial value after 900 fs. On the other hand, the dihedral $C_2'-N_1'-C_6'-C_5'$ varies little until 760 fs and sharply rises to 30° at 860 fs. The variation of the $C_2'-N_1'-C_6'-C_5'$ dihedral angle suggests that interbase interaction leads to deformation of C′ after 760 fs. The strong torsion of C′ gives rise to nonadiabatic transition, which leads to the electronic ground state.

Interesting changes in the C_5-C_6 and $C_5'-C_6'$ bond lengths are observed between 100 and 760 fs. The C_5-C_6 bond length shortens from 1.53 to 1.48 Å, the $C_5'-C_6'$ bond length stretches from 1.38 to 1.42 Å. These variations of bond lengths are closely related to charge transfer, as seen in Figure 6. Before 100 fs, the relatively flat curve of net charge on C molecule suggests that there is no intermolecular charge transfer. Thereafter, about 1.3 electrons transfer from C′ to C; after 760 fs, charge

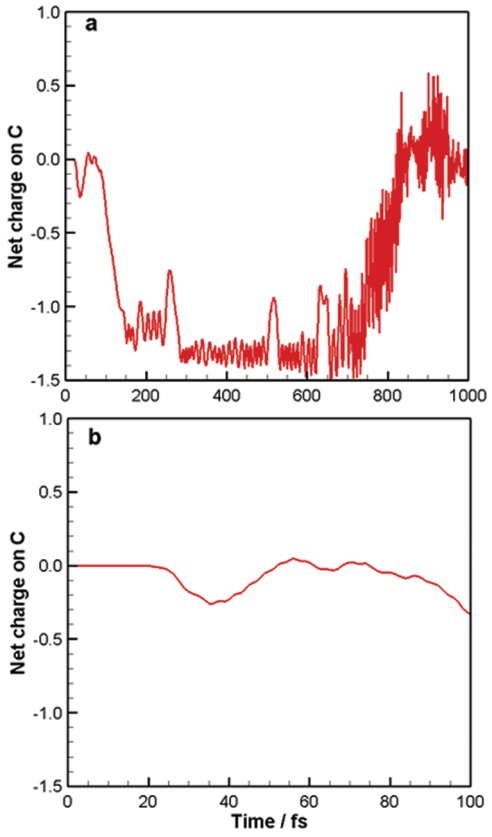

Figure 6. Variations with time of the net charge on C molecule.

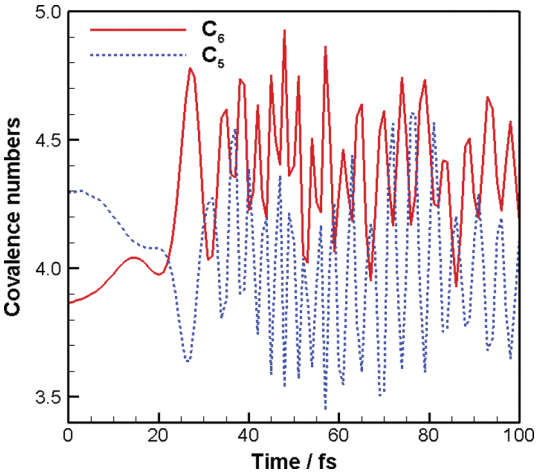

Figure 7. Variations with time of the covalence numbers of (a) C_5 and C_6 and (b) C_5' and C_6'.

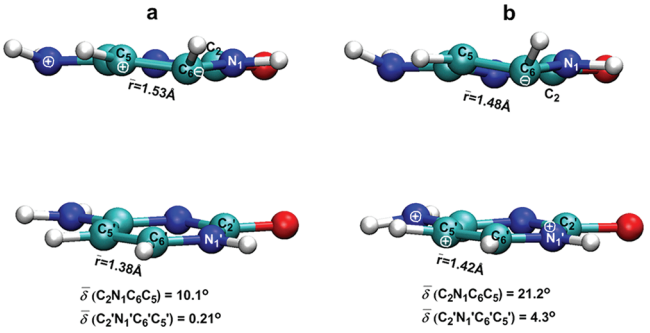

Figure 8. Geometries of (a) the exciton and (b) the excimer .

recombination drives electrons back to C′ and two molecules return to being electrically neutral at the avoided crossing (830 fs). When electrons migrate to C, increasing electronic density between C_5 and C_6 results in a reduced C_5-C_6 bond length because of the increased C_5-C_6 bond order. Conversely, a decrease in electronic density in C′ due to the weakening of $C_5'-C_6'$ π bond is manifestated as an increase in the $C_5'-C_6'$ bond length.

Figure 7 displays the number of valence electrons in C_5, and C_6, the atoms most actively involved in the excitation−deactivation process of pyridines. The valence electrons on these atoms are calculated through the projection of single electronic wave functions to the orbitals of these atoms. Affected by polar of heteroatoms among aromatic nucleus, valence electrons of carbon atoms usually fluctuate about the original value of 4 instead of being exactly equal to 4. For the structure shown in Figure 1, for example, the covalence numbers of C_5 and C_6 are 4.31 and 3.86, respectively. Breaking the C_5-C_6 π bond by laser excitation redistributes the π electrons. As a result, the covalence number of C_5 drops from 4.31 to 3.9 and one of C_6 increases to an average of about 4.5 during the first 100 fs. Because there is minimal electron transfer between the two cytosines during this time period (Figure 6b), this indicates a charge separation within the excited C molecule; in other words, an "exciton" state is formed. The lifetime of this exciton is less than 100 fs, which is consistenet with experimental results.[32]

According to some experimental and theoretical research,[37,58−60] exciton formation tends to precede the evolution to excimer/exciplex. The shortening of C_5-C_6 and elongation of $C_5'-C_6'$, as shown in Figure 4, suggests an exciton state evolving to a charge transfer state (i.e., excimer) after 100 fs. As a consequence of π stacking, the excimer should be formed in a suitable initial intermolecular distance, which is about 3.8 Å by SERID simulation. If the distance between two bases is lager than 3.8 Å, the weaker interaction of bases will lead to a monomer-like deactivation channel via $(S_1/S_0)_{CI}$.

Geometries of the exciton and excimer are shown in Figure 8. The $C_2-N_1-C_6-C_5$ dihedral angle is larger for the excimer. Greater torsion results in a lower LUMO energy (cf. Figures 3 and 5) and higher electron affinity for C, leading to an electron transfer from C′ to C. As mentioned earlier, Figure 6, electrons transport back to C′ (charge recombination) occurs at 760 fs and the avoided crossing occurs at 830 fs; snapshots at these times are shown in in Figure 9. At 760 fs, intermolecular distance has shortened to about 3 Å. Intense interaction at this short distance leads to even larger deformation of C and C′. The $C_2-N_1-C_6-C_5$ and $C_2'-N_1'-C_6'-C_5'$ dihedral angles reach their maximum values at 830 fs. This strong torsion causes a nonadiabatic transition to electronic ground state. For the molecular geometry taken at 830 fs, the C5−C5′ and C6−C6′ distances are 2.11 and 2.13 Å, respectively; these compare favorably with 2.27 and 2.17 Å obtained by CASSCF/CASPT2 calculation at the conical intersection between the lowest excited singlet state and the ground state.[40] This indicates that the avoided crossing found at 830 fs is, indeed, in close proximity to the conical intersection.

dx.doi.org/10.1021/jp207550a |J. Phys. Chem. A 2011, 115, 13291–13297

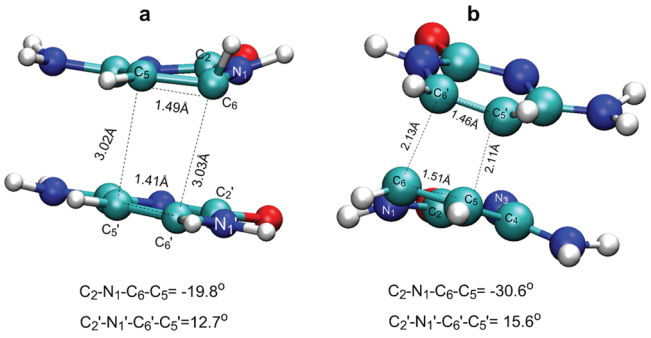

Figure 9. Geometries taken from trajectory at (a) 760 fs and (b) 830 fs, when charge recombination and avoided crossing occur, respectively.

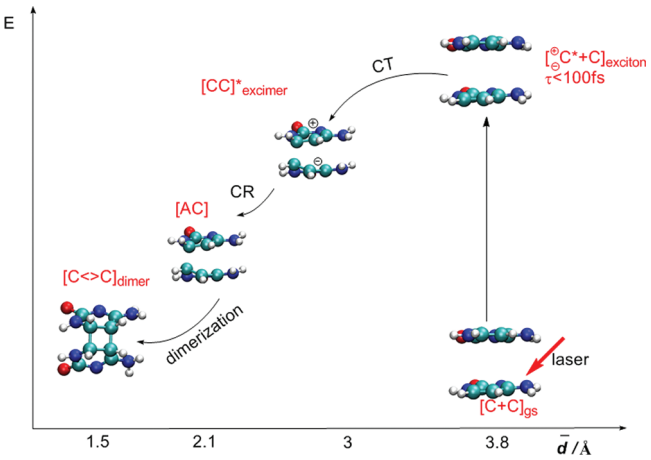

Figure 10. Mechanism of photodimerization reaction of π stacked cytosines system. The abbreviations are interpreted as follows: CT, charge transfer; CR, charge recombination; AC, avoided crossing; gs, ground state.

Figure 10 summarizes the changes in molecular geometry for the representative trajectory. Shortly after application of the laser pulse (<100 fs), a neutral dipolar coupling excited state with ultrashort lifetime, an exciton, is formed. After 120 fs, the twisting of dihedral angle $C_2-N_1-C_6-C_5$ increases the electron affinity of C and leads to a transfer of 1.3 electrons from C′ to C; an excimer is formed. When two bases approach to within a distance of about 3 Å, charge recombination occurs; the stacked cytosines revert to neutral. The system evolves to an avoided crossing due to vibrational coupling of the HOMO and LUMO induced by maximal deformation of C and C′ molecules.

IV. CONCLUSIONS

This paper presents simulation results for the photodimerization of the π-stacked cytosine system following excitation with a laser pulse with 4.1 eV photon energy. Only one cytosine is excited at the beginning. Excitation initially leads to the formation of a charge separated neutral excited state with a lifetime of 100 fs, similar to "Frenkel exciton states" formed by the coupling of $^1\pi\pi^*$ states (which localized on single bases) of proximal nucleobases proposed by Gustavsson, Markovitsi, and coworkers.[30−33] An "excimer state" results from charge transfer that occurs when the interbase distance drops below 3.8 Å. Charge recombination occurs when the interbase distance shortens to about 3 Å, leading to neutral stacked bases that evolve into an avoided crossing prior to deactivation. Geometries taken from avoided crossing is very similar to the S_1/S_0 conical intersection obtained by CASSCT/CASPT2.[40,41] Tortional vibrations ($C_2-N_1-C_6-C_5$ and $C_2'-N_1'-C_6'-C_5'$) play a significant role in vibronic coupling between the HOMO and LUMO and lead to nonadiabatic transition of the molecules to the ground state. Two chemical bonds linking two cytosines are formed soon after the excimer decays to the electronic ground state; the formations of these bonds are synchronous. The lifetime of the C<>C excimer is only hundreds of femtoseconds, significantly shorter than the lifetime of the adenine (A<>A) excimer.[29] It is possible that the weaker conjugate effect caused by smaller aromatic ring of cytosine leads to a less stable, much short-lived excimer. The simulation results provide detailed information on the dynamics of dimerization reactions of stacked cytosines from photon excitation to deactivation and are expected to be helpful in understanding this process.

AUTHOR INFORMATION

Corresponding Author

*E-mail: yusheng.dou@nicholls.edu (Y.D.), fangwh@bnu.edu.cn (W.F.).

ACKNOWLEDGMENT

This work is supported by the National Natural Science Foundation of China (No. 21073242) and Natural Science Foundation Project of CQ CSTC (cstc2011jjA00009).

REFERENCES

(1) Cadet, J.; Sage, E.; Douki, T. *Mutat. Res.* **2005**, *571*, 3–17.
(2) Beukers, R.; Eker, A. P. M.; Lohman, P. H. M. *DNA Repair* **2008**, *7*, 530–543.
(3) Mouret, S.; Baudouin, C.; Charveron, M. *Proc. Natl. Acad. Sci. U. S. A.* **2006**, *103*, 13765–13770.
(4) Melnikova, V. O.; Ananthaswamy, H. N. *Mutat. Res.* **2005**, *571*, 91–106.
(5) Schreier, W. J.; Schrader, T. E.; Koller, F. O.; Gilch, P.; Crespo-Hernández, C. E.; Swaminathan, V. N.; Carell, T.; Zinth, W.; Kohler, B. *Science* **2007**, *315*, 625–629.
(6) Schreier, W. J.; Kubon, J.; Regner, N. *J. Am. Chem. Soc.* **2009**, *131*, 5038–5039.
(7) Douki, T.; Reynaud-Angelin, A.; Cadet, J.; Sage, E. *Biochemistry* **2003**, *42*, 9221–9226.
(8) Zhang, R. B.; Eriksson, L. A. *J. Phys. Chem. B* **2006**, *110*, 7556–7562.
(9) Boggio-Pasqua, M.; Groenhof, G.; Schäfer, L. V.; Grubmüller, H.; Robb, M. A. *J. Am. Chem. Soc.* **2007**, *129*, 10996–10997.
(10) Durbeej, B.; Eriksson, L. A. *J. Photochem. Photobiol. A* **2002**, *152*, 95–101.
(11) Blancafort, L.; Migani, A. *J. Am. Chem. Soc.* **2007**, *129*, 14540–14541.
(12) Johnson, A. T.; Wiest, O. *J. Phys. Chem. B* **2007**, *111*, 14398–14404.
(13) Ravanat, J.-L.; Douki, T.; Cadet, J. *Photochem. Photobiol. B: Biol.* **2001**, *63*, 88–102.
(14) Lee, D. H.; Pfeifer, G. P. *J. Biol. Chem.* **2003**, *278*, 10314–10321.
(15) Douki, T.; Cadet, J. *Biochemistry* **2001**, *40*, 2495–2501.
(16) Cannistraro, V. J.; Taylor, J. S. *J. Mol. Biol.* **2009**, *392*, 1145–1157.
(17) Frederico, L. A.; Kunkel, T. A.; Shaw, B. R. *Biochemistry* **1990**, *29*, 2532–2537.

(18) Eisinger, J.; Guéron, M.; Schulman, R. G.; Yamane, T. *Proc. Natl. Acad. Sci. U. S. A.* **1966**, *55*, 1015–1020.
(19) Birks, J. B. *Nature* **1967**, *214*, 1187–1190.
(20) Serrano-Andrés, L.; Merchán, M.; Borin, A. C. *Chem.—Eur. J.* **2006**, *12*, 6559–6571.
(21) Pecourt, J. M.; Peon, J.; Kohler, B. *J. Am. Chem. Soc.* **2001**, *123*, 10370–10378.
(22) Ismail, N.; Blancafort, L.; Olivucci, M.; Kohler, B.; Robb, M. A. *J. Am. Chem. Soc.* **2002**, *124*, 6818–6819.
(23) Langer, H.; Doltsinis, N. L.; Marx, D. *Chem. Phys. Chem.* **2005**, *6*, 1734–1737.
(24) Barbatti, M.; Lischka, H. *J. Phys. Chem. A* **2007**, *111*, 2852–2858.
(25) Hudock, H. R.; Levine, B. G.; Thompson, A. L.; Satzger, H.; Townsend, D.; Gador, N.; Ullrich, S.; Stolow, A.; Martínez, T. J. *J. Phys. Chem. A* **2007**, *111*, 8500–8508.
(26) Kwok, W. M.; Ma, C.; Phillips, D. L. *J. Am. Chem. Soc.* **2006**, *128*, 11894–11905.
(27) Crespo-Hernández, C. E.; Kohler, B. *J. Phys. Chem. B* **2004**, *108*, 11182–11188.
(28) Middleton, C. T.; de La Harpe, K.; Su, C.; Law, Y. K.; Crespo-Hernández, C. E.; Kohler, B. *Annu. Rev. Phys. Chem.* **2009**, *60*, 217–239.
(29) Schwalb, N. K.; Temps, F. *Science* **2008**, *322*, 243–245.
(30) Bouvier, B.; Dognon, J. P.; Lavery, R.; Markovitsi, D.; Millié, P.; Onidas, D.; Zakrzewska, K. *J. Phys. Chem. B* **2003**, *107*, 13512–13522.
(31) Emanuele, E.; Markovitsi, D.; Millie, P.; Zakrzewska, K. *Chem. Phys. Chem.* **2005**, *6*, 1387–1392.
(32) Onidas, D.; Gustavsson, T.; Lazzarotto, E.; Markovitsi, D. *Phys. Chem. Chem. Phys.* **2007**, *9*, 5143–5148.
(33) Buchvarov, I.; Wang, Q.; Raytchev, M.; Trifonov, A.; Fiebig, T. *Proc. Natl. Acad. Sci. U. S. A.* **2007**, *104*, 4794–4797.
(34) Zgierski, M. Z.; Fujiwara, T.; Lim, E. C. *Chem. Phys. Lett.* **2008**, *463*, 289–299.
(35) Crespo-Hernández, C. E.; Cohen, B.; Kohler, B. *Nature* **2006**, *441*, E8.
(36) Cohen, B.; Hare, P. M.; Kohler, B. *J. Am. Chem. Soc.* **2003**, *125*, 13594–13601.
(37) Takaya, T.; Su, C.; de La Harpe, K.; Crespo-Hernández, C. E.; Kohler, B. *Proc. Natl. Acad. Sci. U. S. A.* **2008**, *105*, 10285–10290.
(38) Crespo-Hernández, C. E.; Cohen, B.; Kohler, B. *Nature* **2006**, *436*, 1141–1144.
(39) Zhang, W.; Yuan, S.; Li, A.; Dou, Y.; Zhao, J.; Fang, W. *J. Phys. Chem. C* **2010**, *114*, 5594–5601.
(40) Roca-Sanjuán, D.; Olaso-González, G.; González-Ramírez, I.; Serrano-Andrés, L.; Merchán, M. *J. Am. Chem. Soc.* **2008**, *130*, 10768–10779.
(41) Serrano-Pérez, J. J.; González-Ramirez, I.; Coto, P. B.; Merchán, M.; Serrano-Andrés, L. *J. Phys. Chem. B* **2008**, *112*, 14096–14098.
(42) Dou, Y.; Torralva, B. R.; Allen, R. E. *J. Mod. Opt.* **2003**, *50*, 2615–2643.
(43) Dou, Y.; Torralva, B. R.; Allen, R. E. *Chem. Phys. Lett.* **2004**, *392*, 352–358.
(44) Graf, M.; Vogl, P. *Phys. Rev. B* **1995**, *51*, 4940–4949. See also: Boykin, T. B.; Bowen, R. C.; Klimeck, G. *Phys. Rev. B* **2001**, *63*, 245314.
(45) Allen, R. E.; Dumitrica, T.; Torralva, B. R. In *Ultrafast Physical Processes in Semiconductors*; Tsen, K. T., Ed.; Academic Press: New York, 2001; Chapter 7.
(46) Ben-Nun, M.; Martínez, T. J. *Adv. Chem. Phys.* **2002**, *124*, 439–512.
(47) Yuan, S.; Dou, Y.; Wu, W.; Hu, Y.; Zhao, J. *J. Phys. Chem. A* **2008**, *112*, 13326–13334.
(48) Yuan, S.; Wu, W.; Dou, Y.; Zhao, J. *Chin. Chem. Lett.* **2008**, *19*, 1379–1382.
(49) Dou, Y.; Hu, Y.; Yuan, S.; Wu, W.; Tang, H. *Mol. Phys.* **2009**, *107*, 181–190.
(50) Yuan, S.; Wang, D.; Bai, M.; Wei, Z.; Meng, P.; Dou, Y. *Journal of Chongqing Univerisity and Telecommunications(Natural Science Edition)* **2009**, *21*, 821–824.
(51) Yuan, S.; Wu, W.; Wen, Z.; Shu, K.; Tang, H.; Dou, Y.; Lo, G. *Mol. Phys.* **2010**, *108*, 3431–3441.
(52) Lei, Y.; Yuan, S.; Dou, Y.; Wang, Y.; Wen, Z. *J. Phys. Chem. A* **2008**, *112*, 8497–8504.
(53) Dou, Y.; Xiong, S.; Wu, W.; Yuan, S.; Tang, H. *J. Photochem. Photobiol. B* **2010**, *101*, 31–36.
(54) Zhang, W.; Yuan, S.; Wang, Z.; Qi, Z.; Zhao, J.; Dou, Y.; Lo, G. *Chem. Phys. Lett.* **2011**, *506*, 303–308.
(55) Yuan, S.; Zhang, W.; Li, A.; Zhu, Y.; Dou, Y. *Acta Phys.—Chim. Sin.* **2011**, *27*, 824–830.
(56) Sharonov, A.; Gustavsson, T.; Carre, V.; Renault, E.; Markovitsi, D. *Chem. Phys. Lett.* **2003**, *380*, 173–180.
(57) González-Ramírez, I.; Roca-Sanjuán, D.; Climent, T.; Serrano-Pérez, J. J.; Merchán, M.; Serrano-Andrés, L. *Theor. Chem. Acc.* **2011**, *128*, 705–711.
(58) Kohler, B. *J. Phys. Chem. Lett.* **2010**, *1*, 2047–2053.
(59) Bittner, E. R. *J. Chem. Phys.* **2006**, *125*, 094909 (1–12).
(60) Improta, R.; Santoro, F.; Barone, V.; Lami, A. *J. Phys. Chem. A* **2009**, *113*, 15346–15354.